# Confinement of a mirror plasma with an anisotropic electron distribution function

A. V. Turlapov

*Physics Department, New York University, 4 Washington Place, New York, New York 10003*

V. E. Semenov

*Institute of Applied Physics, Russian Academy of Science, Ulyanova Street 46, Nizhny Novgorod 603600, Russia*

A theoretical model has been developed for an electron-cyclotron-resonance-heated plasma confinement in a mirror magnetic trap. The model is based on the simultaneous study of noncollisional kinetics of electrons and gas dynamics of ions. At the trap center, the electron velocity distribution function is approximated by bi-Maxwell distribution with two effective temperatures, transverse and longitudinal to the magnetic field. Electrons were assumed to be hotter than ions. Axial distributions of the ambipolar potential and plasma density as well as the ion confinement time have been investigated both numerically and analytically. A simple formula for the lifetime is suggested. Numerical simulations as well as the formula show that the confinement time is heavily dependent on the electron distribution anisotropy and, in the strongly anisotropic case, on ion temperature if the latter is not too small. With increasing anisotropy the ambipolar potential changes qualitatively, acquiring a peak between the trap center and the plug. [S1063-651X(98)09705-0]

PACS number(s): 52.50.Gj, 52.55.Dy, 52.55.Jd

## I. INTRODUCTION

Employment of high-power gyrotrons and magnetrons for electron-cyclotron-resonance (ECR) plasma heating has made it possible to get mirror plasmas with a highly energetic electron component [1–4]. As a result, open magnetic traps with powerful ECR heating (ECRH) are widely used in applied and fundamental research. The traps are basically employed as external ion sources for cyclotron accelerators [5]. In addition, the extracted ion beams are successfully used in atomic and solid-state physics, material science, semiconductor fabrication [5], and ion-beam lithography [6]. Another promising application of ECRH traps is their use as soft-x-ray sources [7,8,4].

Expanding applications of traps with an intense ECRH require an adequate theory of plasma confinement. Powerful ECRH produces a strongly anisotropic electron velocity distribution function (EDF): The mean energy of the motion transverse to the magnetic field is much greater than the energy of the longitudinal motion [9,10]. The most popular models for the plasma lifetime [11–13] do not take into account that the intense heating strongly effects confinement processes. The Pastukhov model [11,12] analyzes electron diffusion into the loss cone of velocity space; only diffusion caused by Coulomb collisions is considered. However, due to intense heating, the electron motion in velocity space is quite different: The prevailing diffusion mechanism is not the Coulomb scattering, but an interaction with the rf field [10]. The Pastukhov model does not consider the latter channel of losses.

The Ryutov-Mirnov gas dynamic trap model [13] considers plasma losses as a gas leakage from a vessel through a nozzle, where the Maxwell EDF is assumed. The model does not take into account that an anisotropic EDF may cause a much bigger lifetime than an isotropic one because of a perfect confinement of large pitch-angle electrons that prevail in an anisotropic case.

The paper proposes a model of plasma confinement under intense ECRH conditions. It is assumed that we know the EDF at the trap center formed by interactions of electrons with the intense resonance field. The use of a model EDF lets us avoid solving a problem of electron diffusion in velocity space caused by the rf field. Within the model framework, ion confinement time, self-consistent profiles of ambipolar potential, and plasma density are deduced by means of analytical estimations and numerical studies.

## II. MODEL DEVELOPMENT

### A. Principles of the model

The model studies a steady-state confinement of ECRH plasma in a mirror magnetic trap (Fig. 1). The steady state results from a balance between two effects: electron-impact ionization of neutral atoms and leakage of the charged particles through the plugs. A two-component plasma (singly charged ions and electrons) is being considered. The magnetic field is assumed to be large enough to neglect radial electron and ion losses.

According to theoretical studies [10], under the powerful ECRH, the EDF at the central part of the trap is stretched along $V_{e\perp}$ [Fig. 2(a)]; $V_{e\parallel}, V_{e\perp}$ are electron velocity compo-
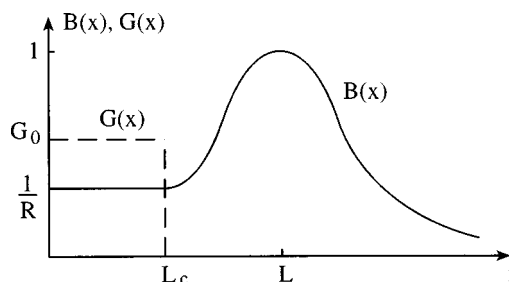


FIG. 1. Axial magnetic induction $B(x)$ profile. The number of neutral atoms ionized in a unit volume per unit time $G(x)$ is not to scale. $x=0$ is a plane of symmetry.
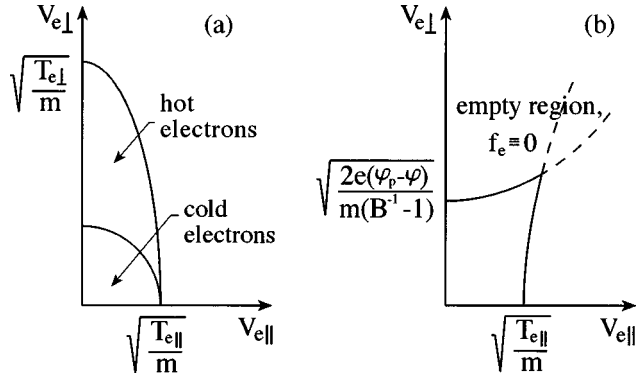
FIG. 2. Electron velocity distribution function (a) at the central cross section and (b) outside the trap at $B < B_0(1 - T_{e\parallel}/T_{e\perp})$.

nents; $\parallel$ and $\perp$ in subscripts designate axial and radial directions. A much greater velocity spread in the radial direction than in the axial one is characteristic for ECR ion source plasmas [9]. Two electron fractions can be distinguished [Fig. 2(a)]: an energetic-hot electron population with mean energy (effective temperature) $T_{e\perp}$ and a cold component with temperature $T_{e\parallel}$. Anisotropy of the distribution is concentrated in the hot fraction, while the cold-electron distribution is isotropic. ECRH plasma experiments give characteristic values $T_{e\perp} = 1 - 50$ keV and $T_{e\parallel} = 10 - 30$ eV [1,2,7].

That anisotropic EDF results from the interaction of electrons with the ECR frequency field [14,10]. The interaction causes electron diffusion in the plane of perpendicular velocities. The rf-induced diffusion is very strong: It fills the loss cone of velocity space even in the absence of the Coulomb collisions and boosts $T_{e\perp}$. Formation of the EDF and plasma confinement are closely linked processes. Here we do not attempt to solve both problems. Upon taking some model for the electron velocity distribution, we do not need to know the detailed mechanism of the electron leak from the trap in order to compute the plasma lifetime. Had we known the mechanism, we could have computed the input rf power required to gain particular electron temperatures $T_{e\perp}$ and $T_{e\parallel}$. We only use the bi-Maxwell model distribution in order to simplify computations. Our basic results can be formulated in terms of characteristic transverse and longitudinal temperatures.

Ion motion is to be described gas dynamically because we are primarily interested in the systems used as ECR ion and soft-x-ray sources. In those applications ions are rather cold $T_{ion} < T_{e\parallel}$ [1,3].

We assume quasineutrality and study plasma both inside and outside the trap. The latter enables us to unambiguously determine the ion velocity in the plug and thereby uniquely compute the ion confinement time and distributions of plasma density and ambipolar potential.

The problem being discussed is close to the problem of ambipolar potential formation in the plug/barrier cell of the tandem mirror machine [15,16] used for fusion research. However, there are two important differences: In the latter problem (i) ions are much hotter and (ii) electron distribution is less anisotropic because electrons may be energetically coupled with ions in the central cell and, because of the large scale of the tandem mirrors, input ECRH power per electron is less than in ECR ion and soft-x-ray sources.

### B. Electron velocity distribution function

Assuming that the ECR-heated zone is located at the central cross section of the trap, we approximate the EDF in that section by a bi-Maxwell distribution [Fig. 2(a)]

$$f_e(x=0,V_{e\parallel},V_{e\perp}) = \exp\left[ -\frac{mV_{e\parallel 0}^2}{2T_{e\parallel}} - \frac{mV_{e\perp 0}^2}{2T_{e\perp}} \right], \quad (1)$$

where $m$ is the electron mass, the node in subscripts designates values at the trap center, $T_{e\parallel}$ and $T_{e\perp}$ are the electron mean energies of the motion parallel and perpendicular to the magnetic field ($x$ axis), respectively, and the normalization constant is omitted. Also $T_{e\parallel}$ and $T_{e\perp}$ can be interpreted as effective temperatures of the cold and hot electrons. Reference [17] exploited a relativistic version of the distribution (1) for electron-cyclotron-emission studies.

Noncollisional electron confinement is assumed ($\lambda_e \gg L$, $\lambda_e$ is the electron mean free path, and $2L$ is the distance between the plugs); the trap is assumed to be adiabatic. Under those conditions $f_e$ depends only on integrals of motion (energy and adiabatic invariant):

$$\frac{mV_{e\parallel}^2}{2} + \frac{mV_{e\perp}^2}{2} - e\varphi = \text{const}, \quad (2a)$$

$$\frac{V_{e\perp}^2}{B} = \text{const}, \quad (2b)$$

where $\varphi$ is the ambipolar potential, $B$ is the normalized magnetic induction [$B(x=L) \equiv B_p = 1$; $p$ in subscripts designates values at the plug], and $-e$ is the electron charge. The integrals (2) let us the compute the EDF at an arbitrary cross section inside the trap:

$$f_e = \exp\left[ -\frac{m}{2T_{e\parallel}}\left( V_{e\parallel}^2 + V_{e\perp}^2 + \frac{2e(\varphi - \varphi_0)}{m} \right) \right. $$
$$\left. + \frac{m}{2T_{e\parallel}}\left( 1 - \frac{T_{e\parallel}}{T_{e\perp}} \right)\frac{B_0 V_\perp^2}{B} \right]. \quad (3)$$

Beyond the plugs we can again compute the EDF using Eq. (2). However, outside we should adjust Eq. (3), taking into account the fact that the large pitch-angle electrons reflect from the plugs and stay inside, i.e., the velocity space has an empty region, in which $f_e \equiv 0$. At $x > L$, relations (2) are only satisfied within one sheet hyperboloid in the velocity space

$$V_{e\perp}^2(B^{-1} - 1) - V_{e\parallel}^2 = -\frac{2e(\varphi - \varphi_p)}{m}, \quad (4)$$

which sets the boundary of the empty region. In the velocity space inside the hyperboloid, the EDF is determined by Eq. (3), while outside of it $f_e \equiv 0$ [Fig. 2(b)].

Generally speaking, at the central cross section, the EDF differs from the model distribution (1), proposed above. However, the difference, if any, does not cause a substantial error in our numerical simulations because we only use the EDF to compute the dependence of the plasma density on $\varphi$ and $B$, i.e., we are only interested in the zeroth moment of the EDF.

## C. Gas dynamics of ions

We will assume that ions are being contained in the gas dynamic regime ($\lambda_{ii} \ll L$; $\lambda_{ii}$ is the ion mean free path for ion-ion collisions). Hence ion collective motion can be described gas dynamically:

$$\frac{\partial}{\partial x_j}(N v_j) = G, \tag{5a}$$

$$\frac{\partial}{\partial x_k}(N v_j v_k + p \, \delta_{jk}) = -\frac{e}{M} N \frac{\partial \varphi}{\partial x_j} \qquad j,k=1,2,3. \tag{5b}$$

Here $N$, $\mathbf{v}$, $M$, and $p$ are the ion density, velocity, mass, and pressure, respectively; $\delta_{jk}$ is the Kronecker delta function; and $G$ is the number of ions and electrons being born in a unit volume per unit time. The generation source $G$ will be neglected near and beyond the plugs [$G(x>L_G)=0$, $L_G < L$]. In order to take into account the magnetic field, Eq. (5) needs to be supplied with an additional requirement: Ions can only move along the magnetic lines of force.

The ion pressure is approximated as an ideal gas pressure

$$p = N T_{ion}. \tag{6}$$

The ion flow is conjectured to be isothermal [$T_{ion}(x) \equiv \text{const}$], i.e., we neglect gas cooling when it runs along a tube of flux.

It is convenient to convert from the three-dimensional description to a quasi-one-dimensional one, assuming that the magnetic induction lines are almost parallel to the trap axis. In order to do that, we need to integrate Eq. (5) over a trap cross section and substitute Eq. (6) into Eq. (5b). The equations obtained are written in normalized variables

$$\frac{d}{dx}(Snu) = gS, \tag{7a}$$

$$\frac{d}{dx}[Sn(u^2 + u_T^2)] = -u_\parallel^2 nS \frac{d\Phi}{dx} + u_T^2 n \frac{dS}{dx}, \tag{7b}$$

where $\Phi \equiv e\varphi/T_{e\parallel}$ is the normalized ambipolar potential, $n \equiv N/N_p$, $u \equiv v/c_s$, $c_s^2 \equiv (T_{ion}+T_{e\parallel})/M$ is the ion "sound speed" squared, $u_T$ is the normalized ion thermal speed, $u_T^2 \equiv T_{ion}/(T_{ion}+T_{e\parallel})$, $u_\parallel^2 \equiv 1 - u_T^2$, $g \equiv G/c_s N_p$ is the normalized density of the ion generation source, and $S(x)$ is a trap cross-sectional area. In that normalization, the model becomes a two-parameter one (if the magnetic system parameters remain unchanged, the solution only depends on $T_{e\perp}/T_{e\parallel}$ and $T_{ion}/T_{e\parallel}$).

Equations (7) are two in number but have three unknown functions: $n(x)$, $u(x)$, and $\Phi(x)$. We obtain the third equation by assuming plasma quasineutrality, $N=N_e$, inside and outside the trap. Integration of the EDF over the velocity space yields

$$n = \frac{1-\kappa}{1-\kappa B^{-1}} \exp(\Phi) \quad \text{at} \quad x \lesssim L, \tag{8a}$$

$$n = \frac{1-\kappa}{1-\kappa B^{-1}}\left[ \exp(\Phi) - \sqrt{\frac{1-B}{1-\kappa}} \exp\left( \Phi \frac{1-\kappa}{1-B} \right) \right]$$

$$\text{at} \quad x \gtrsim L. \tag{8b}$$

$\kappa \equiv (1 - T_{e\parallel}/T_{e\perp})/R$ ($R \equiv B_p/B_0 = 1/B_0$ is the trap mirror ratio) and the ambipolar potential is chosen to be zero in the plugs ($\Phi_p = 0$). If the EDF is strongly anisotropic, $\kappa \simeq 1/R$. $B$ and $S$ are given functions, connected by the condition of magnetic flux preservation $S(x) = S_p/B(x)$.

From Eqs. (8a) and (8b) one can see how vital it is to take into account the empty region in velocity space. If we expanded Eq. (8a) into the $x > L$ region (i.e., did not take the empty region into account), we would acquire an infinite density blowup at $B = \kappa$.

## D. Boundary conditions

The set of equations (7) and (8) is closed. In order to complete the mathematical model, the equations need to be supplied with boundary conditions. Let the solution meet some physically backed restrictions: $\Phi(x)$, $n(x)$, and $u(x)$ are smooth everywhere (except maybe the point $x = L_G$, at which the ion generation is abruptly turned off) and

$$n(x \to \infty) \to 0. \tag{9}$$

The symmetry of the model with respect to the central cross section together with the smoothness requirement yields

$$u_0 = 0. \tag{10}$$

Solutions to Eqs. (7) and (8a) and to Eqs. (7) and (8b) should be matched in the plug at the boundary $x = L$. Again, from the smoothness requirement we have

$$u_p = 1, \tag{11}$$

i.e., in the plug, the ion gas dynamic velocity turns into the "sound speed." A proof of the boundary condition (11) can be found in Appendix A. Despite the EDF being non-Maxwellian, we deduced boundary condition, which is usual for the problem of gas flow from a vessel through a nozzle.

One more very important feature of the boundary condition is that it is in agreement with the Bohm criterion [18]. In reality, the plasma is confined in some finite volume. The plasma beam, extracted from the trap, hits a wall of a vacuum chamber or a surface to be processed that is more or less absorbing. According to the Bohm criterion, ions should approach the sheath, which shields the plasma from the wall, with a velocity greater than or equal to the ion sound speed. From the boundary condition (11) we obtain a supersonic plasma flow beyond the plugs that fulfills the Bohm criterion. Outside the trap, $c_s$ is a true ion sound speed, without any quotation signs, because cold electrons dominate in that region and $T_{e\parallel}$ may be treated as a true electron temperature.

Now, having the boundary conditions (10) and (11), one can integrate Eq. (7) outside the ionization region:
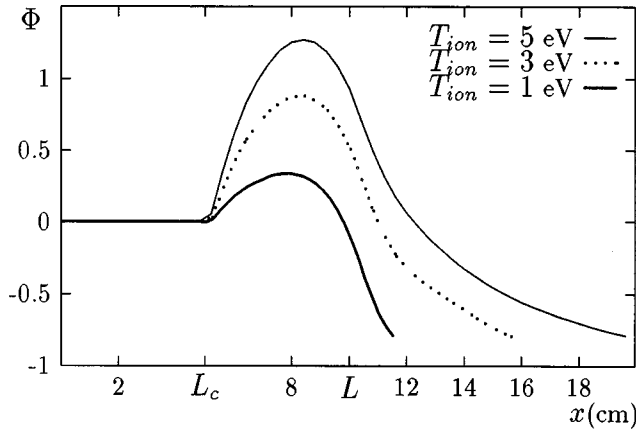
$$un = B, \tag{12a}$$

FIG. 3. Normalized ambipolar potential at intense ECRH ($T_{e\parallel}$ = 10 eV, $T_{e\perp}$ = 1 keV; here the potential is chosen to be zero at the trap center). There is a slight potential dropoff at $0 \leqslant x \leqslant L_c$, which is indistinguishable at that scale.

$$\frac{1}{2}(u^2 - 1) + u_T^2 \ln(n) + u_\parallel^2 \Phi \equiv 0. \quad (12b)$$

Further, the integrals will be used to estimate the height of the potential peak, plasma density, and ion lifetime. In addition, the boundary conditions (10) and (11) let us calculate the normalization constant, ion density in the plug

$$N_p = \frac{1}{S_p c_s} \int_0^L G(x) S(x) dx.$$

### III. TYPICAL MODEL INPUTS AND PARAMETER SPACE INVESTIGATED

Equations (7) and (8) with the boundary conditions (9)–(11) enable one to perform a numerical simulation. The model inputs are the (i) geometry of the trap [magnetic induction distribution $B(x)$], (ii) density of the ionization source $G(x)$, (iii) ratio of the hot- and cold-electron temperatures $T_{e\perp}/T_{e\parallel}$, and (iv) ratio of the ion and cold electron temperatures $T_{ion}/T_{e\parallel}$. Figure 1 displays the magnetic induction distribution in the trap we studied. In the center, it has a constant magnetic field region of length $2L_c$. We took $L_c = \frac{1}{2}L$ and $R = 3$.

The ion generation was assumed to be constant at $x \leqslant L_G \leqslant L$ and zero at $x > L_G$ (Fig. 1). We simulated at different $L_G \geqslant L_c$ and found that the solution $(\Phi(x), n(x), u(x))$ is almost independent of $L_G$. For the results given below, $L_G = L_c$. The following range of temperature ratios was investigated: $T_{e\perp}/T_{e\parallel} = 1$–$100$ ($T_{e\perp} = 10$ eV–10 keV, $T_{e\parallel} = 10$–$100$ eV), $T_{ion}/T_{e\parallel} = 0.01$–$0.5$.

### IV. ANALYTICAL AND NUMERICAL RESULTS

#### A. Self-consistent ambipolar potential

Numerical simulation, based on Eqs. (7) and (8) with the boundary conditions (9)–(11), lets us build a self-consistent distribution of the ambipolar potential in space inside and outside the trap. Figure 3 shows simulation results for the parameters characteristic for ECRH plasmas. In all cases, we clearly see the ambipolar potential peak.

Formation of the peak can be understood from the following qualitative reasoning. The hot electrons [see Fig. 2(a)] are perfectly confined at the central part of the trap and do not penetrate deep into the plugs because of their large pitch angles. Since the EDF is strongly anisotropic, the cold electrons are few at the trap center (about $T_{e\parallel}/T_{e\perp}$ of the whole number of electrons), but the losses from the region are determined just by the cold electrons. If the ion temperature $T_{ion}$ is higher than a certain threshold, the number of ions leaving the central part of the trap, due to thermal motion, exceeds the number of such electrons. Hence, in order to balance the ion and electron fluxes from the region, there should appear an ambipolar field, which reduces leakage of ions and stimulates electron losses from the central part of the trap. Thus it should be a region between the center and the plug where the ambipolar potential increases outward from the trap center (see Fig. 3).

Near the plug inside the trap, on the contrary, cold electrons dominate. In this region, the ambipolar field must slow down electrons and speed up ions; otherwise, due to thermal motion, electrons would leave the trap faster than ions. Hence, near the plugs the potential drops off. Thus, self-consistently with electron and ion flow balancing, we obtained the ambipolar potential maximum (peak) between the center and the plug.

At $T_{e\parallel}/T_{e\perp} \ll 1$, $u_T \ll 1$, we can estimate the height of the peak $\Delta\Phi \equiv \Phi_{peak} - \Phi(x = L_c)$ as

$$\Delta\Phi = u_T^2 \ln\left[\frac{T_{e\perp}}{T_{e\parallel}}(R-1)u_T\right] + \left(\frac{T_{e\parallel}}{T_{e\perp}}\right)^2 \frac{1}{(R-1)^2 2e}. \quad (13)$$

The derivation of the estimation as well as of the condition (14) can be found in Appendix B; here and further $e$ is the base of the natural logarithm.

The peak cannot be observed if the ions are cold enough. For the plasma with the strongly anisotropic EDF, the peak vanishes at

$$\frac{T_{ion}}{T_{e\parallel}} \leqslant \left(\frac{T_{e\parallel}}{T_{e\perp}}\right)^2 \frac{1}{(R-1)^2 e}. \quad (14)$$

The latter condition is almost unattainable, for instance, at $T_{e\parallel} = 10$ eV, $T_{e\perp} = 1$ keV, and $R = 3$; the peak vanishes at $T_{ion} = 10^{-4}$ eV $\simeq 1$ K. Thus, under powerful ECRH conditions, the ambipolar potential must always have a maximum between the plug and the central cross section.

In Fig. 4 we have plotted the peak height $\Delta\Phi$ versus the ion normalized thermal speed squared $u_T^2$. The dependence can be perfectly approximated by a straight line

$$\Delta\Phi(u_T^2) = u_T^2 A,$$

as it is seen from the estimation (13). However, according to our numerical results, the slope $A$ of that line is bigger than $\ln[(T_{e\perp}/T_{e\parallel})(R-1)u_T]$.

One may prove analytically that in the case of the isotropic EDF ($T_{e\perp}/T_{e\parallel} = 1$) the potential peak cannot be observed at any $T_{ion}$. The potential decreases monotonically when going from the trap center to infinity (Fig. 5). It was found numerically that under weak ECRH ($T_{e\perp}/T_{e\parallel} \sim 1$), the peak
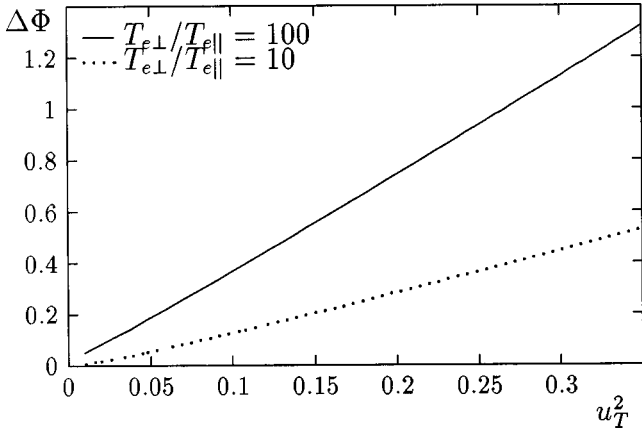
FIG. 4. Height of the ambipolar potential peak vs normalized ion thermal speed squared $u_T^2 \equiv T_{ion}/(T_{ion}+T_{e\parallel})$.

appears at some threshold value of $T_{ion}/T_{e\parallel}$. For instance, at $T_{e\perp}/T_{e\parallel}=1.10$, the threshold is $T_{ion}/T_{e\parallel}=0.97$.

Within the model framework, one can investigate the behavior of the potential far from the trap ($B \to 0$). Equations (8b) and (12) yield the estimation

$$\Phi \propto -\ln|\ln B| \tag{15}$$

and the potential slowly decreases to $-\infty$. Virtually, the estimation (15) is valid only until the quasi-one-dimensional approximation is fair, the adiabatic invariant (2b) is being preserved, and ion gas dynamics works.

If one modeled a trap with the Maxwell EDF not taking into account the empty region in the velocity space [in order to perform it Eq. (8) should be changed to $n = \exp \Phi$], the analogous estimation would read

$$\Phi \propto \ln B.$$

References [7,3] used the potential profile with the peak as a hypothesis. They suggested a model profile with two parameters: the height of the peak and the potential dropoff at infinity; these two parameters were computed using plasma experimental data ($T_{ion}, T_{e\parallel}, T_{e\perp}$, and the hot-electron density [7]; $T_{ion}$, the ion lifetime, and the ion density [3]). The
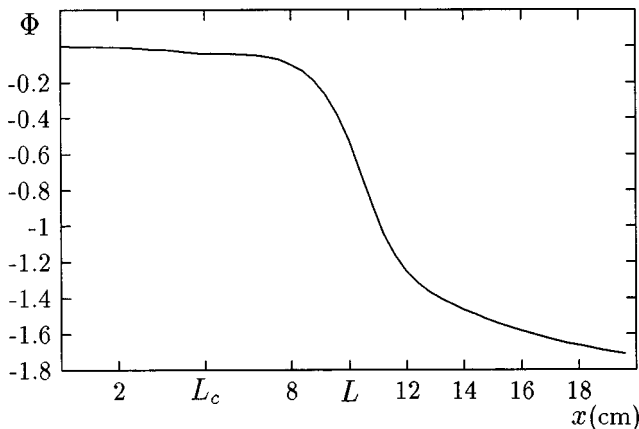
model presented not only deduces the characteristic potential configuration, but also computes its exact spatial distribution.

### B. Density profile

The plasma density profile is very much dependent on the EDF anisotropy, i.e., on the ratio $T_{e\perp}/T_{e\parallel}$. At large $T_{e\perp}/T_{e\parallel}$, the majority of electrons are hot electrons with large pitch angles. They are perfectly confined at the central part of the trap and do not deeply penetrate into the plug. Thus the plasma with a strongly anisotropic EDF is basically being confined at the trap center, in the region of almost constant magnetic induction (Fig. 6). The localization of hot electrons at that trap part has been observed experimentally [2].

Having neglected in Eqs. (8a) and (12b) that $u(x=L_c)$ and $n(x=L_c)$ differ from $u_0=0$ and $n_0$, respectively, one can estimate the normalized plasma density at the trap center as

$$n_0 = \sqrt{e}\left[\frac{T_{e\perp}}{T_{e\parallel}}\left(1-\frac{1}{R}\right)+\frac{1}{R}\right]^{1-u_T^2}. \tag{16}$$

In the weak ECRH case, the EDF is almost isotropic and the plasma distribution over the trap is more uniform (Fig. 7). At



FIG. 6. Normalized plasma density at intense ECRH ($T_{e\parallel}=10$ eV, $T_{e\perp}=1$ keV).



FIG. 5. Normalized ambipolar potential for isotropic EDF ($T_{e\perp}=T_{e\parallel}=10$ eV, $T_{ion}=1$ eV; here the potential is chosen to be zero at the trap center).
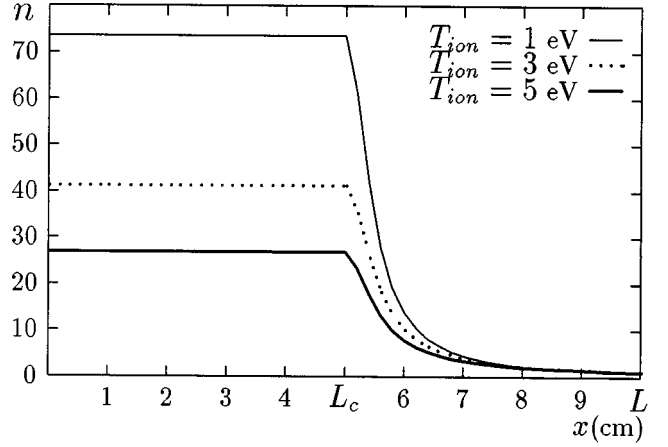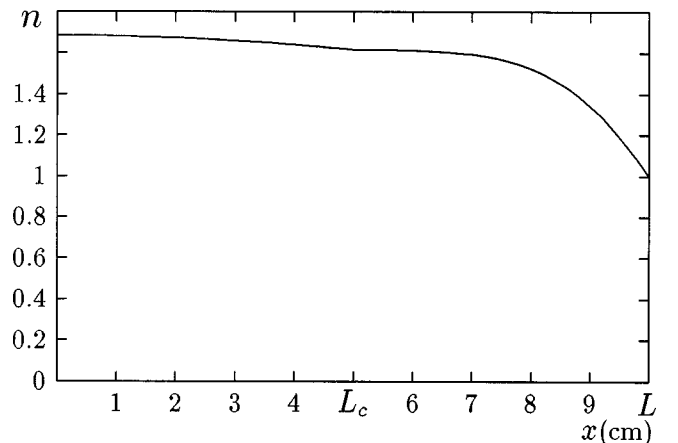


FIG. 7. Normalized plasma density for isotropic EDF ($T_{e\perp}=T_{e\parallel}=10$ eV, $T_{ion}=1$ eV).

$T_{e\perp}/T_{e\parallel}=1$, the estimation (16) yields $n_0=\sqrt{e}$. Far from the trap ($B\rightarrow 0$), the density is proportional to $B$ up to a logarithmically slow factor. Thus, at infinity $n$ vanishes and thereby the boundary condition (9) is satisfied.

### C. Ion confinement time

Let us define the confinement time as the number of ions in the trap divided by the ion flux through the plug

$$\tau=\frac{\int_0^L NS(x)dx}{N_p S_p c_s}.$$

If the central trap region with a constant magnetic field is long enough ($L_c\lesssim L$), $\tau$ can be computed analytically:

$$\tau=\frac{L_c R}{c_s}\sqrt{e}\left[\frac{T_{e\perp}}{T_{e\parallel}}\left(1-\frac{1}{R}\right)+\frac{1}{R}\right]^{1-u_T^2}. \tag{17}$$

The Ryutov-Mirnov gas dynamic trap model [13] assumes an isotropic electron velocity distribution ($T_{e\parallel}=T_{e\perp}$) and estimates the ion lifetime as $\tau_{RM}=L_c R/c_s$. Obviously, $\tau_{RM}$ factors out from formula (17), which yields, in the isotropic case,

$$\tau=\frac{L_c R}{c_s}\sqrt{e}\simeq\tau_{RM}. \tag{18}$$

It is not surprising that formula (17) embraces $\tau_{RM}$ as a special case because both our and the Ryutov-Mirnov models describe ions gas dynamically and assume $T_{ion}$ to be constant in the whole bulk of plasma. $\tau$ tremendously differs from $\tau_{RM}$ under a high-power ECRH. In order to picture the difference we introduce dimensionless normalized lifetime

$$t\equiv\tau\left[\frac{L_c R}{c_s}\sqrt{e}\right]^{-1}.$$

If the EDF is strongly anisotropic and the central trap region with constant $B$ is long enough, then

$$t\simeq\left[\frac{T_{e\perp}}{T_{e\parallel}}\right]^{1-u_T^2}\quad\text{or}\quad \ln t\simeq(1-u_T^2)\ln\frac{T_{e\perp}}{T_{e\parallel}}, \tag{19}$$

whence we see that $t$ is only dependent upon the distribution anisotropy and upon the ratio of the ion and cold-electron temperatures. In Fig. 8 we have plotted the results of numerical computations of $t$ in comparison with the estimation (19). The graph clearly shows that the normalized lifetime rises as the anisotropy of the distribution increases and as the ion temperature (to be more precise, the ratio $T_{ion}/T_{e\parallel}$) drops off. Comparing the factored out normalized lifetime with the Ryutov-Mirnov one, we can see that the dependence on the ion temperature is very different in the isotropic and anisotropic cases. At a weak ECRH, it is the quite slow square-root dependence (18), while at an intense heating it is exponential law (19).
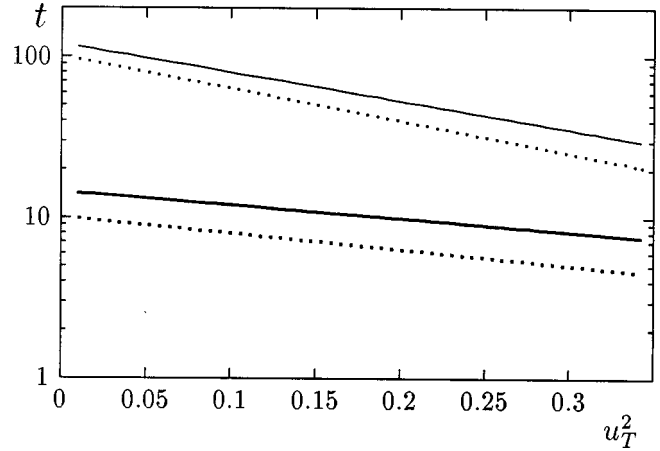


FIG. 8. Normalized confinement time on a logarithmic scale vs normalized ion thermal speed squared $u_T^2\equiv T_{ion}/(T_{ion}+T_{e\parallel})$. A comparison of the estimation (19) (dotted lines) with numerical calculations (solid lines) is shown for different electron temperatures: $T_{e\perp}/T_{e\parallel}=100$ (thick lines) and $T_{e\perp}/T_{e\parallel}=10$ (thin lines).

### D. Model limitations

Now, having studied properties of the model developed, we are in a position to elaborate upon the model limitations $\lambda_{ii}\ll L$ and $\lambda_e\gg L$. Let us write these restrictions on the mean free paths for the plasma in the plug, expressing $\lambda_{ii}$ and $\lambda_e$ in terms of the magnetic system parameters, temperatures, and plasma density [$L$(cm); $T_{ion},T_{e\parallel}$(eV); and $N_p$(cm$^{-3}$)]. At the plug, these restrictions are equivalent to the respective expressions

$$\frac{1}{2}\times 10^{12}\times\frac{T_{ion}^2}{N_p}\ll L, \tag{20a}$$

$$10^{12}\times\frac{T_{e\parallel}^2}{N_p}\gg L. \tag{20b}$$

If $\lambda_{ii}\ll L$ is true in the plug then it is true in the whole trap because the density monotonically decreases outward from the center. Thus Eq. (20a) is the condition of ion gas dynamics use in the model developed. The condition (20b) of the noncollisional electron pass through the plug is independent of $T_{e\perp}$ because cold electrons dominate in the plug. It follows from Eqs. (16) and (20b) that $10^{12}T_{e\perp}^2/N_0\gg L$, i.e., when the condition (20b) is satisfied, hot-electron confinement is also noncollisional. We do not demand $\lambda_e\gg L$ for isotropically distributed cold electrons at the central part of the trap because their collisions do not change the EDF. Thus Eqs. (20) are sufficient (but not necessary) conditions for applications of the model suggested.

It is worth noting that the validity of some of our results does not depend on whether or not the ion mean free path is small compared to the trap scale. At $T_{ion}\ll T_{e\parallel}$, one may set $T_{ion}=0$ and sufficiently accurately compute the plasma density and ion confinement time under any conditions on $\lambda_{ii}$, including the $\lambda_{ii}\gg L$ case. This can be explained in the following physical arguments.

At $\lambda_{ii}>L$, ion gas dynamic equations (5) still hold, but instead of $p\delta_{jk}$ in Eq. (5b) we have the diagonal pressure tensor $p_{jk}=NT_{ion,j}(x)\delta_{jk}$; $T_{ion,1}(x)\equiv T_{ion\parallel}(x)$ and

$T_{ion,2}(x) = T_{ion,3}(x) \equiv T_{ion\perp}(x)$. Now, in place of the uniform ion temperature $T_{ion}$, we have second moments of the ion velocity distribution, which are position dependent. This position dependence may be very strong because at $\lambda_{ii} > L$ unconfined regions of the ion velocity space are not filled and dimensions of such a region acutely depend on whether it is related to the point inside or outside the electrostatic potential well. Now, in order to compute the height of the potential peak, $T_{ion}$ in formula (13) must be replaced with some functional of $T_{ion\parallel}(x)$ and $T_{ion\perp}(x)$. Our model cannot compute the value of the functional and therefore is unable to predict $\Delta\Phi$ with any suitable precision because $\Delta\Phi$ is almost proportional to $T_{ion}$ or its substitute [see Eq. (13)], i.e., when we make a big error guessing the value of the functional, we make the same big error in the height of the peak. As we can see now, the potential is very much dependent on the validity of the gas dynamic approximation for ions. In order to find the ambipolar potential distribution for the plasma with a large ion mean free path, the kinetic description of ions should be used, as it was done in computations for plug/barrier cells of the tandem mirror machine [16]. Alternatively, after calculation of the plasma lifetime within our model, the Pastukhov formula [11] might be applied to find $\Delta\Phi$.

In the $T_{ion} \ll T_{e\parallel}$ limit, unlike the height of the peak, the plasma density and confinement time are weakly dependent on $T_{ion}$ [see Eqs. (16) and (17)] and thus can be computed in the approximation $T_{ion}/T_{e\parallel} \simeq \text{const} = 0$ for any ion mean free path. That approximation will not bring about a substantial error. Of course, when we write $T_{ion} \ll T_{e\parallel}$ for the $\lambda_{ii} < L$ case, $T_{ion}$ should be understood as some characteristic energy rather than as a true temperature because the ion velocity distribution is non-Maxwellian in this case.

## V. CONCLUSION

A model for the confinement of plasma with the anisotropic EDF, given at the trap center, has been developed. The use of the model EDF lets us solve the confinement problem without specifying a mechanism of electron losses.

The results obtained indicate that the distribution anisotropy strongly affects the plasma lifetime, density profile, and shape of the ambipolar potential. Under intense ECRH, the plasma is basically contained at the central part of the trap, unlike the more or less uniform distribution for $T_{e\perp}/T_{e\parallel} \sim 1$. As $T_{e\perp}/T_{e\parallel}$ exceeds a certain threshold, the self-consistent potential profile changes qualitatively: A peak appears between the center and the plug. It is very important to take into account the ion thermal motion when computing the height of the peak because its height increases with the increase of $T_{ion}/T_{e\parallel}$ and the peak does not appear at all when the ratio is zero. In experiments with a high-power ECRH, the peak should be present at all achievable ion temperatures. The enhancement of the confinement time with increasing EDF anisotropy (at constant $T_{ion}/T_{e\parallel}$) is evident. The plasma lifetime, computed for the particular case of an isotropic EDF, is about equal to the lifetime in the Ryutov-Mirnov gas dynamic trap model [13].

The model presented can be generalized for the description of a plasma with ions of different charges. As before, each type of ion can be separately described by equations of quasi-one-dimensional gas dynamics (7). Apparently, the ion source ($g$) will depend on the densities of ions. The electron density will remain dependent on the magnetic induction and on the potential in the same fashion as given by Eq. (8). Obtaining a new boundary condition in the plug requires further studies, but there is hope that it will remain as simple as it is: In the plug, the gas dynamic velocity of each type of ion will be equal to the respective "sound speed" (the speed will depend on the ion charge).

## APPENDIX A: PROOF OF THE BOUNDARY CONDITION (11)

Solutions to Eqs. (7) and (8a) and to (7) and (8b) must be smoothly matched in the plug at $x = L$. The boundary condition $u_p = 1$ can be found in the following fashion.

Equations (7) and (8a) yield, at $x < L$,

$$n' = -\frac{1}{1-u^2}\left[2ug - nu^2\frac{S'}{S} - nu_\parallel^2\frac{S'}{S_0/(1-T_{e\parallel}/T_{e\perp})-S}\right], \quad \text{(A1)}$$

where the prime stands for $d/dx$. It is evident from Eq. (A1) that if $u$ reaches 1 before the plug then $n'$ goes to infinity. Thus $u_p \leq 1$.

Let $u_p < 1$. Then $n'_p = 0$. From $n'_p = 0$ and Eq. (8a), we obtain $\Phi'_p = 0$. Let us expand the solution in a power series of $\xi \equiv x - L$ ($\alpha$ and $\beta$ are constants independent of $\xi$):

$$B = 1 - \beta\xi^2 + o(\xi^2), \qquad \Phi = -\alpha\xi^2 + o(\xi^2).$$

Expansion of Eq. (8b) up to first order reads

$$n = 1 - \xi\sqrt{\frac{\beta}{1-\kappa}}\exp\left(-\frac{\alpha}{\beta}(1-\kappa)\right) + o(\xi),$$

whence $n'_p \neq 0$, i.e., we have a contradiction to the smoothness requirement on $n$ and $\Phi$. At $u_p = 1$ the solution is smooth. Consequently, $u_p = 1$.

## APPENDIX B: DERIVATION OF THE ESTIMATION (13) FOR THE PEAK HEIGHT AND OF THE CONDITION (14) FOR THE PEAK DISAPPEARANCE

We start up from Eqs. (8a) and (12). Excluding $n$ from them we obtain

$$u = \frac{B-\kappa}{1-\kappa}\exp(-\Phi), \quad \text{(B1)}$$

$$\frac{1}{2}(u^2-1) + \Phi + u_T^2\ln\frac{1-\kappa}{1-\kappa B^{-1}} = 0. \quad \text{(B2)}$$

Differentiating Eqs. (B1) and (B2) with respect to $x$ and equating $\Phi'_{peak} = 0$ give

$$u_{peak}^2 = u_T^2 \frac{\kappa}{B_{peak}}. \tag{B3}$$

From Eq. (B2) the height of the peak $\Delta\Phi \equiv \Phi_{peak} - \Phi_c$ can be expressed as

$$\Delta\Phi = \frac{1}{2}(u_c^2 - u_{peak}^2) + u_T^2 \ln\frac{1 - \kappa B_{peak}^{-1}}{1 - \kappa B_c^{-1}}, \tag{B4}$$

where the subscript $c$ refers to point $x = L_c$. Equation (B4) has two unknown values: $u_c$ and $B_{peak}$. To compute them, we put Eqs. (B1) and (B2) together and, excluding $\Phi$, obtain

$$\ln\frac{B - \kappa}{u} = \ln(1 - \kappa) + \frac{1}{2}(1 - u^2) + u_T^2 \ln\frac{B(1 - \kappa)}{B - \kappa}, \tag{B5}$$

which is of course true both at $x_{peak}$ and at $L_c$. Assuming that $u_T \ll 1$ and $T_{e\parallel}/T_{e\perp} \ll 1$, we get from Eq. (B5), at $x = L_c$,

$$u_c = \frac{T_{e\parallel}}{T_{e\perp}} \frac{1}{\sqrt{e}(R - 1)}. \tag{B6}$$

At $x_{peak}$, substituting Eq. (B3) into Eq. (B5) and again applying the same requirements on $u_T$ and $T_{e\parallel}/T_{e\perp}$, we can compute a linear in $u_T$ departure of $B_{peak}$ from $\kappa$:

$$B_{peak} - \kappa = u_T\sqrt{e}(1 - \kappa). \tag{B7}$$

Assembling Eqs. (B3), (B4), (B6), and (B7), one finally obtains the estimation (13).

Now we turn to the proof of the condition (14) of peak disappearance. We can rewrite Eq. (B7) as

$$B_{peak} = B_0 + \frac{1}{R}\left[u_T\sqrt{e}(R - 1) - \frac{T_{e\parallel}}{T_{e\perp}}\right]. \tag{B8}$$

$B_{peak} - B_0 \geq 0$ because $B_0$ is the minimum of the magnetic field in the trap. Hence the peak vanishes as the value in square brackets in Eq. (B8) turns into zero, which gives us the threshold condition (14). One may check that when the condition (14) is satisfied, the estimation (13) reads $\Delta\Phi = 0$.

---

[1] M. E. Mauel, Phys. Fluids **27**, 2899 (1984).

[2] V. N. Bocharov *et al.*, Voprosy Atomnoi Nauki i Tekhniki—Termoyadernyi Sintez (The Problems of Atomic Science and Technology—Thermonuclear Fusion) **3**, 64 (1985) (in Russian).

[3] C. C. Petty, D. L. Goodman, D. K. Smith, and D. L. Smatlak, J. Phys. (Paris) Colloq. **50**, C1-783 (1989).

[4] S. V. Golubev, Yu. Ya. Platonov, S. V. Razin, and V. G. Zorin, J. X-Ray Sci. Technol. **6**, 244 (1996).

[5] M. Sekiguchi, Rev. Sci. Instrum. **67**, 1606 (1996).

[6] V. G. Dudnikov, Rev. Sci. Instrum. **67**, 915 (1996).

[7] J. H. Booske, F. E. Aldabe, R. F. Ellis, and W. D. Getty, J. Appl. Phys. **64**, 1055 (1988).

[8] H. R. Garner, T. Ohkawa, A. M. Howald, A. W. Leonard, L. S. Peranich, and J. R. D'Aoust, Rev. Sci. Instrum. **61**, 724 (1990).

[9] G. Melin, E. Bourg, P. Briand, and R. Geller, J. Phys. (Paris) Colloq. **50**, C1-727 (1989).

[10] S. V. Golubev, V. E. Semenov, E. V. Suvorov, and M. D. Tokman, in *Proceedings of International Workshop on Strong Microwaves in Plasmas, Moscow, 1993,* edited by A. G. Litvak (Institute of Applied Physics, Russian Academy of Science, Nizhny Novgorod, 1994), Vol. 1, p. 347.

[11] V. P. Pastukhov, Nucl. Fusion **14**, 3 (1974).

[12] F. Najmabadi, R. W. Conn, and R. H. Cohen, Nucl. Fusion **24**, 75 (1984).

[13] D. D. Ryutov, Plasma Phys. Controlled Fusion **28**, 191 (1986).

[14] E. V. Suvorov and M. D. Tokman, Sov. J. Plasma Phys. **15**, 540 (1989).

[15] T. Tamano, Phys. Plasmas **2**, 2321 (1995).

[16] I. Katanuma, Y. Kiwamoto, Y. Tatematsu, K. Ishii, T. Saito, K. Yatsu, and T. Tamano, Phys. Plasmas **4**, 2532 (1997).

[17] C. M. Celata, Nucl. Fusion **25**, 35 (1985).

[18] K.-U. Reimann, J. Phys. D **24**, 493 (1991).